



## Dynamic implications of discontinuous recrystallization in cold basal ice: Taylor Glacier, Antarctica

D. Samyn,<sup>1</sup> A. Svensson,<sup>2</sup> and S. J. Fitzsimons<sup>3</sup>

Received 14 June 2006; revised 7 December 2007; accepted 4 March 2008; published 23 August 2008.

[1] Crystallographic investigations have been conducted of cold ( $-17^{\circ}\text{C}$ ) debris-bearing ice from the base of an Antarctic outlet glacier (Taylor Glacier). The 4-m-thick sequence studied has been retrieved from a 20-m-long tunnel dug from the glacier snout and has been analyzed with an automatic ice fabric analyzer (AIFA). The top and bottom of the sequence consists of clean meteoric ice (englacial facies), whereas alternating debris-rich and clean bubbly ice layers are found in the middle part (stratified facies). Ice from the englacial facies displays a polygonal texture and a strong c-axis clustering toward the vertical, denoting recrystallization through “subgrain rotation” (SGR). In contrast, clean ice from the stratified facies shows SGR fabrics which are delimited at the contact with debris-rich layers by large, interlocking grains organized in ribbons. These two distinct textures within the stratified facies are associated with looser c-axis patterns at the scale of single thin sections, which is interpreted as resulting from “migration recrystallization” (MR). The change from SGR to MR trends marks a clear increase in grain boundary and nucleation kinetics (hence the term “discontinuous recrystallization”) and may be associated with strain localization at rheological interfaces during basal ice genesis. Analogies with bottom ice from deep polar ice sheets, where temperature is commonly higher than at the studied site, are highlighted. Two recrystallization scenarios are proposed, accounting for the development of both types of fabrics. It is shown that by controlling the repartition of stress and strain energy within basal ice, the rheology of debris-bearing ice layers plays a decisive role in recrystallization dynamics at structural interfaces. We also demonstrate how the same recrystallization regimes may occur in cold glaciers and temperate ice sheets, provided that strain accumulation has been high enough in the former. This challenges the common belief that migration fabrics observed in bottom ice from deep ice sheets are exclusive to warm, stagnant, annealed ice.

**Citation:** Samyn, D., A. Svensson, and S. J. Fitzsimons (2008), Dynamic implications of discontinuous recrystallization in cold basal ice: Taylor Glacier, Antarctica, *J. Geophys. Res.*, 113, F03S90, doi:10.1029/2006JF000600.

### 1. Introduction

[2] Crystallographic investigations have been conducted in various types of ice bodies, which has raised the awareness of the importance of fabric analysis in understanding ice dynamics. Most of what is known on the development of ice fabrics and the evolution of glacier and ice sheet dynamics comes from the study of deep polar ice cores [e.g., Gow and Williamson, 1976; Langway *et al.*, 1988; Thorsteinsson *et al.*, 1995]. The large time periods spanned by the cores and the high resolution of proxies enclosed have

indeed made it possible to directly correlate the occurrence of specific events in the glacier history with the formation of explicit crystal fabrics. This has led to significant progress in the reconstruction of ice masses through time and to the knowledge of how these masses react to changes in the global environment.

[3] Of particular interest in this context is the role played by the “basal zone” in ice rheology. “Basal ice” corresponds to the ice zone present at the sole of a glacier or an ice sheet. Its study is crucial in glaciology since the basal zone directly reflects the interactions between the glacier substrate and bulk glacier ice [e.g., Lawson, 1979; Souchez and Lorrain, 1991]. Basal ice is generally rich in debris of varying granulometry, concentration, arrangement, and origin [e.g., Lawson, 1979; Hubbard and Sharp, 1989]. This debris has been shown to have a strong influence on fabric anisotropy [e.g., Holdsworth, 1974; Langway *et al.*, 1988; Cuffey *et al.*, 2000], which can in turn contribute to strain partitioning at the base of glaciers and ice sheets [e.g., Fitzsimons *et al.*, 2001; Samyn *et al.*, 2005a].

<sup>1</sup>Department des Sciences de la Terre et de l'Environnement, Faculte des Sciences, Universite de Bruxelles, Brussels, Belgium.

<sup>2</sup>Department of Geophysics, Niels Bohr Institute for Astronomy, Geophysics, and Physics, University of Copenhagen, Copenhagen, Denmark.

<sup>3</sup>Department of Geography, University of Otago, Dunedin, New Zealand.

However, the recent discovery of deep “clean ice” (i.e., ice devoid of any visible debris) displaying heterogeneous crystal fabrics in the basal zone of several deep drilling sites in polar regions (e.g., EDML, Berkner Island, Dome C, Siple Dome, NGRIP) has emphasized the fact that the presence of debris alone cannot account for all observed enhanced basal deformation. Besides, this basal clean ice generally shows the occurrence of what is known as migration recrystallization, i.e., it is characterized by large, interlocking, strain-free grains, which strongly contrasts with what can be found in upper layers [Gow and Williamson, 1976; Alley, 1988; Budd and Jacka, 1989]. This mechanism of recrystallization may also be viewed as “discontinuous” in terms of grain boundary kinetics (see section 5). Although these migration/discontinuous recrystallization layers potentially record the oldest environmental archives at an ice body, very few studies have dealt with the physical conditions underlying this type of recrystallization.

[4] In order to gain a better understanding of the relationships between stress, strain, debris properties, and the mechanisms of recrystallization within basal ice at cold conditions (i.e., below  $\sim -10^{\circ}\text{C}$ ), we focus in this paper on ice fabrics from the basal zone of the margin of Taylor Glacier, Antarctica, where migration recrystallization was observed. After a brief summary of the basic concepts related to the recrystallization of ice in glaciers and ice sheets, we report the evolution of ice crystal fabrics (i.e., c-axis orientation patterns) and textures (i.e., size and arrangement) in the sampled sequence. We then investigate the strain and recrystallization regimes experienced by the studied ice, paying particular attention to the conditions under which discontinuous recrystallization occurred. The role of debris-rich ice layers is highlighted in this regard. Special emphasis is also placed on analogs found with ice fabrics from deep polar ice sheets.

## 2. Ice Recrystallization

### 2.1. Dislocations, Recovery, and Recrystallization

[5] One of the most striking features related to the plasticity of ice is its low crystal symmetry, which can lead to strong viscoplastic anisotropy [Azuma, 1994; Castelnau et al., 1998]. This structural anisotropy is particularly relevant in the context of ice mass flow. For conditions found in glaciers and ice sheets, ice ductility is driven by the glide of dislocations, which occurs preferentially along the basal plane of crystals (basal slip). These dislocations are linear structural defects produced under stress that enable the polycrystal to deform plastically. Part of the mechanical work done by the motion of dislocations is stored as internal strain energy. When dislocations accumulate sufficiently so that they begin to entangle and interact within individual crystals, strain, and thus flow, is hampered. The polycrystal is then said to work harden. The process by which dislocation clusters are overcome and glide space is found to sustain the necessary deformation is known as recovery. In fact, recovery implies the reduction of dislocation density and the rearrangement of dislocations into subboundaries (or low-angle grain boundaries) [Gottstein and Mecking, 1985]. The latter form planar arrays of dislocations that delineate subgrains, i.e., grain portions with basal plane misorientation of a few degrees as compared to the parent

grain. This leads to a lower energy configuration and thus reduces internal strain energy.

[6] Recrystallization is another efficient mechanism for releasing the internal free energy accumulated during deformation [e.g., Barber, 1985]. It involves the spatial rearrangement of grain boundaries [Means, 1983] and the formation and/or migration of high-angle grain boundaries [Vernon, 1981]. This generally leads to the growth of new grains at the expense of older ones [Urai et al., 1986; Alley, 1988]. Recrystallization can occur either during deformation (dynamic recrystallization) or when deformation has eased or stopped (postdynamic, or static recrystallization). It can also occur solely as a result of increased temperature (annealing). In geology, two end-member mechanisms of dynamic recrystallization are generally distinguished: rotation recrystallization and migration recrystallization [e.g., Guillopé and Poirier, 1979; Poirier, 1985], which are described below.

### 2.2. Recrystallization Regimes in Polycrystalline Ice

[7] Through the study of deep ice cores, it is generally acknowledged that the development of ice fabrics in glaciers and ice sheets results from the accumulation of strain and is achieved through distinct recrystallization processes:

[8] 1. Normal grain growth leads to an increase of grain size with ice age following a parabolic (Arrhenius) relation, as shown by Gow [1969] at Byrd Station, Antarctica. This process controls the grain size evolution in the upper layers of glaciers and ice sheets and is driven by the reduction of grain boundary free energy [Gow and Williamson, 1976; Alley, 1988; Ralph, 1990]. Fabrics are generally isotropic in the upper layers, and their pattern should not be affected by normal grain growth.

[9] 2. With increasing strain and stress in deeper layers, rotation recrystallization takes over from normal grain growth and leads to the formation of subgrains as a result of dislocation gathering [e.g., Budd and Jacka, 1989; Thorsteinsson et al., 1995]. The misorientation of subgrains with parent grains progressively increases with deformation, leading to the polygonization (i.e., division) of preexisting grains. Data reanalysis by Durand et al. [2008] showed that this process was likely to occur in the very first hundreds of meters from NGRIP ice core. This process has also been proposed to counteract normal grain growth below 400 m at Byrd Station [Gow and Williamson, 1976; Alley et al., 1995] and below 650 m in the GRIP ice core in Greenland [Castelnau et al., 1998]. These depths correspond to about 20% of the respective total ice sheet thickness. C-axes are generally clustered in this regime, as a result of the increased number of slightly misoriented grains.

[10] 3. In the deepest layers of some glaciers and ice sheets, coarse, recovered, interlocking grains with smooth grain boundaries and dispersed c-axes occur. This is the migration recrystallization field, extending up to the pressure-melting point. Temperature, which enhances the migration rate of grain boundaries between dislocation-free and deformed grains, is considered as the main control [Kamb, 1959; Gow and Williamson, 1976; Alley, 1988; Budd and Jacka, 1989]. This regime would operate only above a critical temperature lying between about  $-13^{\circ}\text{C}$  [Gow and Williamson, 1976] and  $-10^{\circ}\text{C}$  [Duval and Castelnau, 1995].

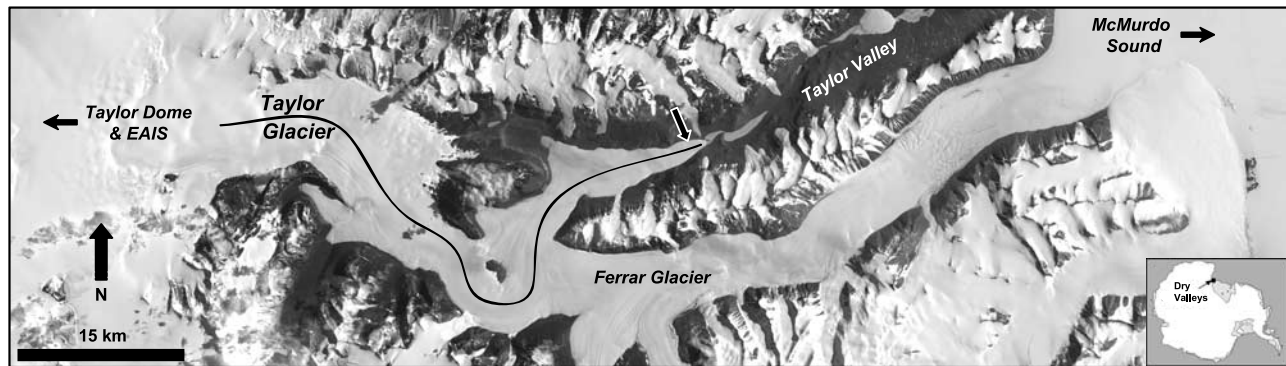


**Figure 1.** Landsat (NASA) image of Taylor Glacier complex, Antarctica. The arrow at the left margin of the glacier denotes the sampling site. The overall orientation of the tunnel according to the glacier snout geometry is given by the arrow direction.

[11] It has been shown that the crystal fabrics resulting from the recrystallization regimes described above can be influenced by the presence of impurities. Solutes will not have a direct effect on crystal size, since they can only reduce grain boundary mobility [Weiss *et al.*, 2002]. Solid particles, however, may reduce crystal size by reducing the driving force for grain growth through grain boundary pinning depending on their size, location, and distribution [Baker, 1978; Alley *et al.*, 1986; Langway *et al.*, 1988]. This pinning effect by solid particles can be overcome under conditions of high driving forces, stress or temperature.

[12] In summary, temperature, stress, strain, and the presence of debris are recognized as the main factors controlling the recrystallization of ice. These factors tend to fluctuate mostly at the base of glaciers and ice sheets [e.g., Anderton, 1974; Gow and Williamson, 1976; Alley, 1988; Budd and Jacka, 1989], which has therefore the potential to generate significant fabric, and thus flow, variability in this zone. These parameters will be investigated here in relation to the transformation of fabrics in cold, debris-bearing ice from the base of Taylor Glacier, Antarctica.

### 3. Field Site and Methods

[13] Taylor Glacier is an outlet glacier from the East Antarctic Ice Sheet, draining continental ice from Taylor Dome toward McMurdo Sound (Figure 1). Taylor Glacier is believed to be polythermal [Robinson, 1984; Hubbard *et al.*, 2004], that is, parts of the basal zone would be perennially cold while other parts would be perennially warm. The mean annual surface temperature at the glacier snout is close to  $-17^{\circ}\text{C}$  [Robinson, 1984], and the lower ablation zone is acknowledged to be cold based [Calkin, 1974]. The frontal margin of the glacier is a 20-m-high ice cliff facing a perennially ice-covered lake (Lake Bonney).

[14] During the 1999–2000 austral summer, a 20-m-long tunnel was excavated 1.4 km upstream from the glacier snout (Figures 1 and 2). A 4-m-deep shaft was dug at the end of this tunnel in order to examine and recover a series of ice blocks (each  $\sim 30 \times 20 \times 10$  cm) from a linear profile extending up-glacier from the margin. The excavated sequence (Figure 4) was at the homogeneous temperature of  $-17^{\circ}\text{C}$ . Although the bottom of the shaft did not reach the bedrock, investigations conducted in 1998–1999 in

another tunnel close to the one discussed here (S. J. Fitzsimons, unpublished data, 1999) suggest that the bedrock was within a few meters of the shaft floor.

[15] Thin sections were prepared along the sequence using a microtome and a diamond wire saw [Tison, 1994] for debris-poor and debris-rich ice, respectively. Mean thin section dimensions were about 80 (H)  $\times$  70 (L) mm. Ice crystal orientations were measured at the Niels Bohr Institute (University of Copenhagen, Denmark) by means of an automatic ice fabric analyzer (AIFA) (Figure 3) developed by D.S. Russell-Head (University of Melbourne, Australia). The analytical procedure followed has been adapted from Wilson *et al.* [2003], Svensson *et al.* [2003] and Samyn *et al.* [2005b].

[16] The method allows for either semi-automatic or manual processing. Though more repetitive and time consuming than the semi-automatic way, manual processing was chosen for this work. The latter method consists of loading the digitalized section image acquired with the AIFA into separate analysis software (Investigator), and then spotting individual crystals on the image to get their c-axis orientation. This “spotting” technique proved to be

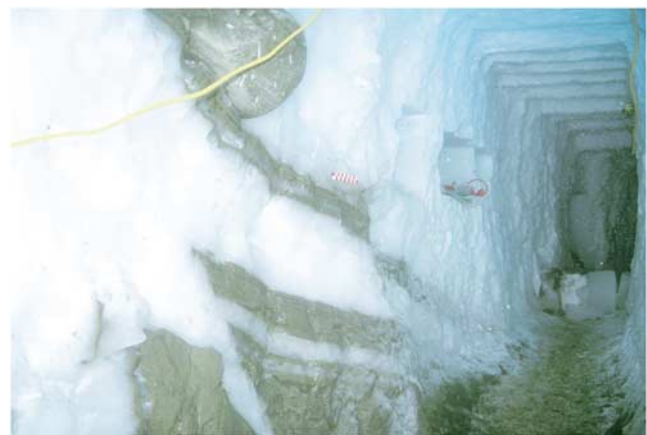


**Figure 2.** Entrance of the subglacial tunnel ( $\sim 20$  m long,  $\sim 2$  m high). Dipping of the clean and debris-rich ice layers toward inner glacier ( $\sim 15^{\circ}$ ) is clearly visible. Note the meter-scale boulder overlying a debris-rich ice layer at the forefront. Ice in the tunnel is at the homogeneous temperature of  $-17^{\circ}\text{C}$ .

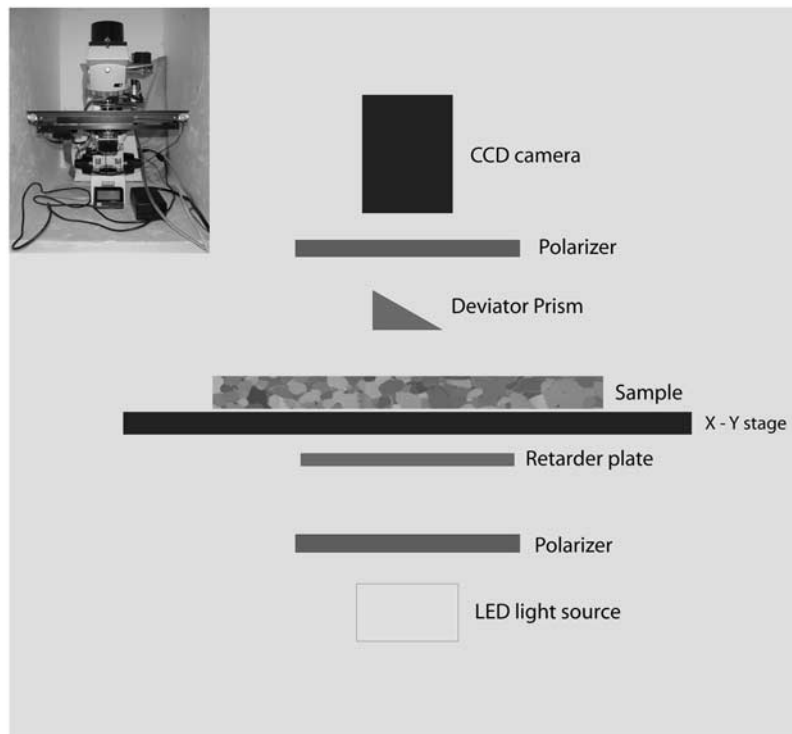


**Figure 3.** Schematized components of the automatic c-axis analyzer used at the Niels Bohr Institute (University of Copenhagen, Denmark).

more appropriate for the case of (1) ice with a high debris content, as thin section preparation with the diamond wire saw may produce tiny grooves that may become assimilated to structural features on scanning and (2) highly interlocking crystals, for which the intricacy of grain boundaries eventually makes automated centering of crystals awkward [Samyn, 2005].

[17] Given that a poor statistical representation of modal fabrics is obtained when large crystals are present, only composite fabrics with different grain types at thin-section scale were considered in this work. To visualize the ice fabric evolution, fabric diagrams are provided in Figures 5 and 6 and statistical parameters ( $R$  and eigenvalues) in Tables 1 and 2. Here,  $R$  values define the “orientation strength” [Wallbrecher, 1978] and can be derived by treating each c-axis measured on thin sections as a unit vector. When  $R$  is equal to 0%, all c-axes are distributed in a random way. When  $R$  is equal to 100%, all c-axes are

**Table 1.** Statistical Parameters Related to the Basal Ice Sequence of Taylor Glacier<sup>a</sup>

Fabric Set	Height (m)	$R$ (%)	$S_3$	$S_2$	$S_1$	$I$
a	3.88	85.10	0.02	0.09	0.89	0.03
b	3.47	84.29	0.02	0.10	0.88	0.02
c	3.32	86.00	0.02	0.09	0.89	0.03
d	2.77	51.88	0.09	0.13	0.78	0.12
e	2.69	69.46	0.03	0.18	0.79	0.04
f	2.55	61.89	0.04	0.21	0.75	0.05
g	1.08	55.12	0.14	0.22	0.65	0.21
h	1.02	45.60	0.12	0.32	0.57	0.21
i	0.48	88.90	0.02	0.04	0.94	0.02
j	0.23	90.15	0.01	0.04	0.95	0.01

<sup>a</sup>These parameters were calculated from 100 crystals randomly selected on representative sections from the englacial facies (a–c, i–j) and from the laminated subfacies (d–h).

clustered into a single vertical maximum. Information on the flow symmetry can be gained by intercomparison of the normalized eigenvalues ( $S_1, S_2, S_3$ ) of the second order orientation tensor. These eigenvalues are given in Table 1. The largest eigenvalue correspond to the eigenvector to which most c-axes are parallel [Woodcock, 1977]. Similar values for  $S_1, S_2, S_3$  denote an isotropic fabric, while  $0 \leq S_3 \cong S_2 \leq 1/6$  and  $2/3 \leq S_1 \leq 1$  denote a single maximum. A useful index to describe the fabrics observed is the isotropy index defined as  $I = S_3/S_1$ , that ranges from 0 (clustered c-axes) to 1 (isotropic c-axis distribution) [Hockey, 1970].

#### 4. Results

[18] The sampled 4-m-thick basal ice sequence has been described by Samyn *et al.* [2005b]. The stratigraphy of the basal zone (Figure 4) exhibits two contrasting facies: (1) an englacial facies, consisting of clean bubbly ice, and (2) a stratified facies, characterized by a generally high debris content but internally composed of debris-rich bands interspersed with clean bubbly ice layers near the contact with the englacial facies. The englacial facies was determined on the basis of the ice bubble content, petrography, and gas content. The stratified facies was divided into two subfacies to account for its variability in debris content: (1) the massive subfacies, where debris concentration is close to

**Table 2.** Mean Statistical Parameters for the Englacial Facies ( $N = 5$ ) and the Laminated Subfacies ( $N = 5$ )

Ice Type	Mean $R$ (%)	Mean $S_3$	Mean $S_2$	Mean $S_1$	Mean $I$
Englacial	86.89	0.02	0.07	0.91	0.02
Laminated	56.79	0.08	0.21	0.71	0.13

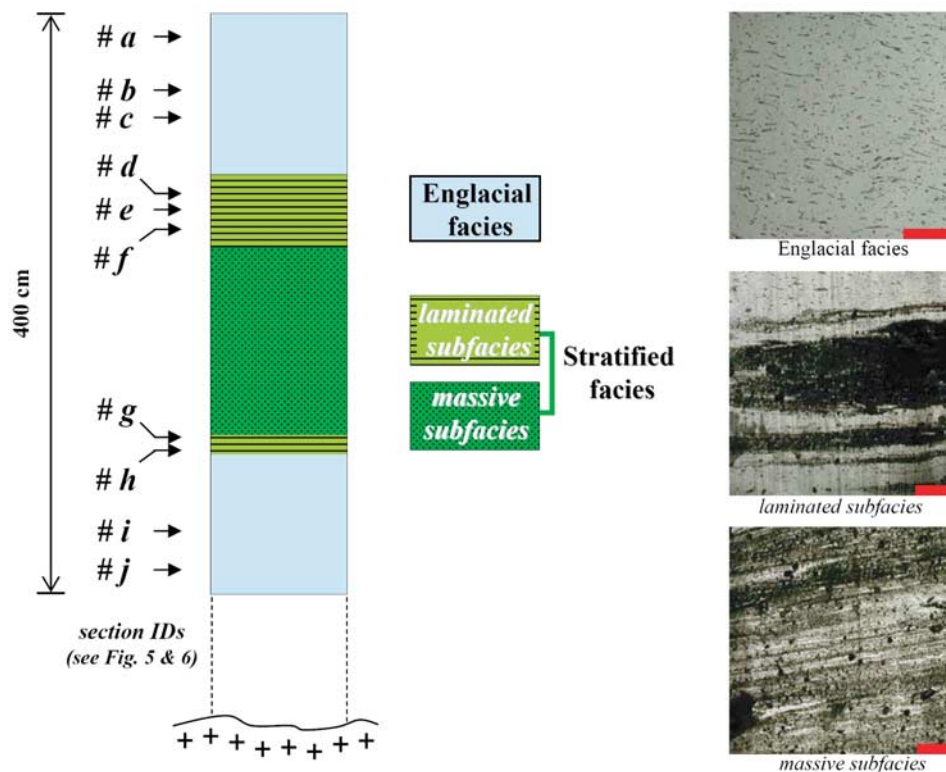


**Figure 4.** Schematized basal ice sequence at the left snout margin of Taylor Glacier, Antarctica. The sequence was sampled from the back wall of the tunnel. Lowercase letters refer to the location within the sequence of the fabric sets provided in Figures 5 and 6 and Tables 1 and 2.

saturation throughout, and (2) the laminated subfacies, where debris-rich layers alternate with clean bubbly ice layers. The whole stacked sequence is dipping  $\sim 15^\circ$  in glacier, as observed at the entrance of the tunnel (Figure 2). We describe below the petrography of the stratigraphical units of interest in this study (i.e., the englacial facies and the laminated subfacies). The respective crystal fabrics are presented in Figure 5. Note that the c-axis orientations of the ice crystals can be identified directly from the processed images by the use of a standard color code (Figure 5k).

#### 4.1. Englacial Facies

[19] The bubbles enclosed in this facies present a high aspect ratio (i.e., the ratio between their diameter and their length is between 0.2 and 0.1) and are aligned parallel to bulk stratification. The ice crystals are generally polygonal, with a mean crystal size of 2.2 mm (e.g., Figures 5i and 5j). When present, silt-sized debris concentrates into 1-mm-thick debris layers parallel to the general stratigraphy. Samyn *et al.* [2005b] showed that the englacial facies is made up of glacier ice formed by firmification.

[20] Schmidt diagrams (Figures 6a, 6b, 6c, 6i, and 6j) show that a tight single-pole fabric, in which very few crystal axes deviate from the vertical, is present. This single-pole fabric is also indicated by large  $R$  and  $S_1$  values (Figure 7, Table 2). It is worth noting from the Schmidt

diagrams that a slight maximum can occur along the flow direction and beyond the  $45^\circ$  inner circle.

#### 4.2. Laminated Subfacies

[21] The stratigraphy of the laminated subfacies is marked by a characteristic sharp compositional banding, with clean bubbly ice layers alternating with debris-rich, bubble-poor ones. Individual debris-rich bands are a few millimeters to a few centimeters thick, and are mostly made up of a silt-to-sand matrix (debris content ranges from 30 to 50% by volume). The clean ice layers from this subfacies are generally similar to the englacial facies: the bubbles are highly elongated parallel to the ice foliation, the crystals show a granular texture, and most c-axes are subparallel to each other ( $R \sim 80\%$ ). At the contact with debris-rich bands, however, the clean ice layers show a sharp increase in crystal size (up to  $28 \times 6$  mm) and aspect ratio (up to  $>4$ ) (Figures 5d, 5g, 5h, and Figure 8). The crystals then present highly interlocked, smooth, lobate grain boundaries as well as a relatively well-defined subrectangular outline relative to elsewhere in the profile (Figure 8). These elongate crystals (which eventually show deformation lamellae and subgrains under polarized light) define distinctive linear features, which we refer to as “ice crystal ribbons,” in which the crystal longest dimensional axes are similarly oriented parallel to the local ice foliation. These conspicu-

**Figure 5.** (a–j) Representative portions of vertical thin sections from the basal ice sequence. Each crystal has been given a specific color to allow for direct appreciation of the c-axis orientations (analysis of orientation axes diagrams). (k) A color code is provided for azimuth and dip identification. Vertical trending axes are in blue, and horizontal ones are in orange. Debris laminations appear in dark gray in Figures 5d, 5g, and 5h. Square dimensions:  $2 \times 2$  cm<sup>2</sup>.

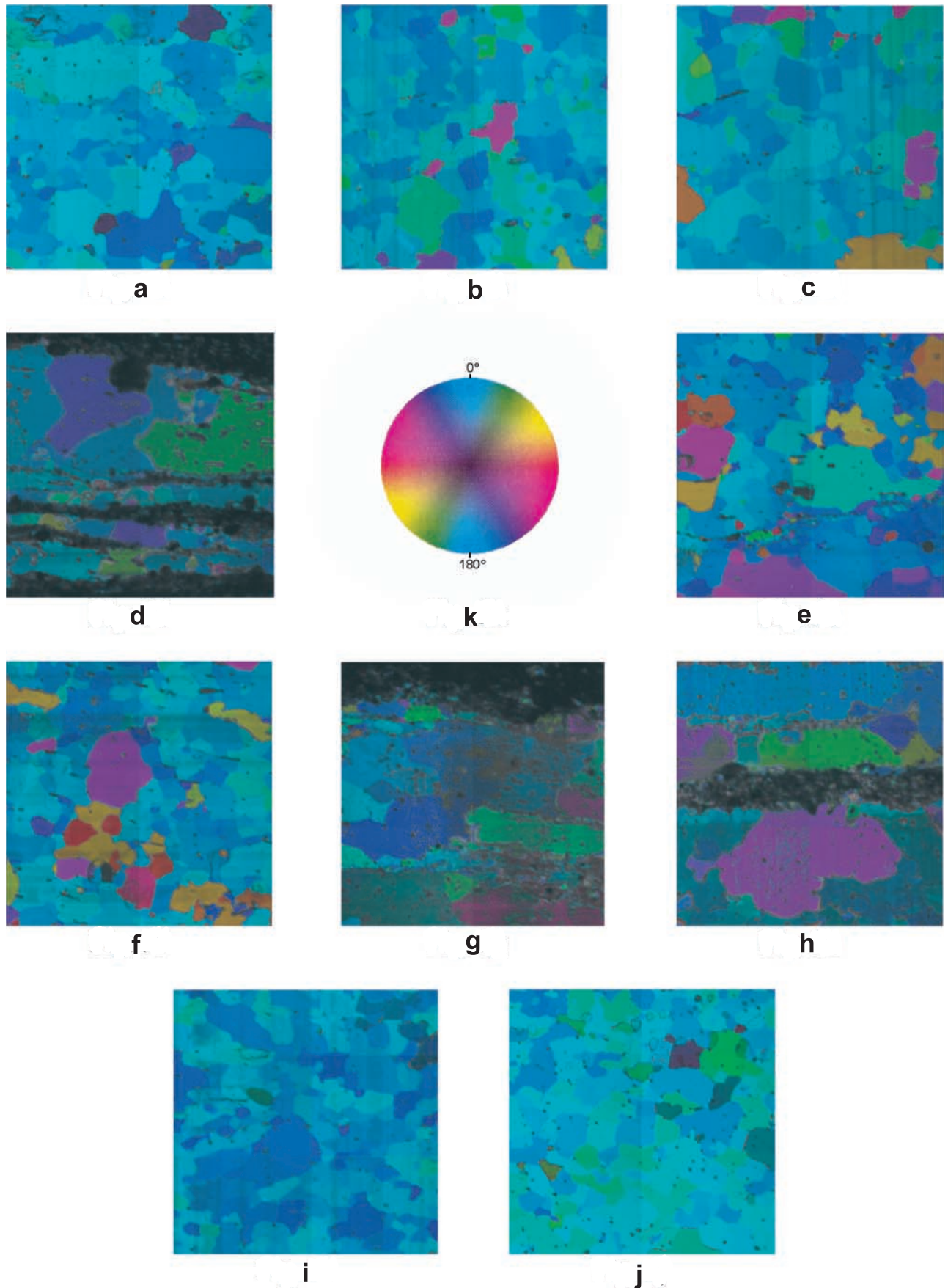
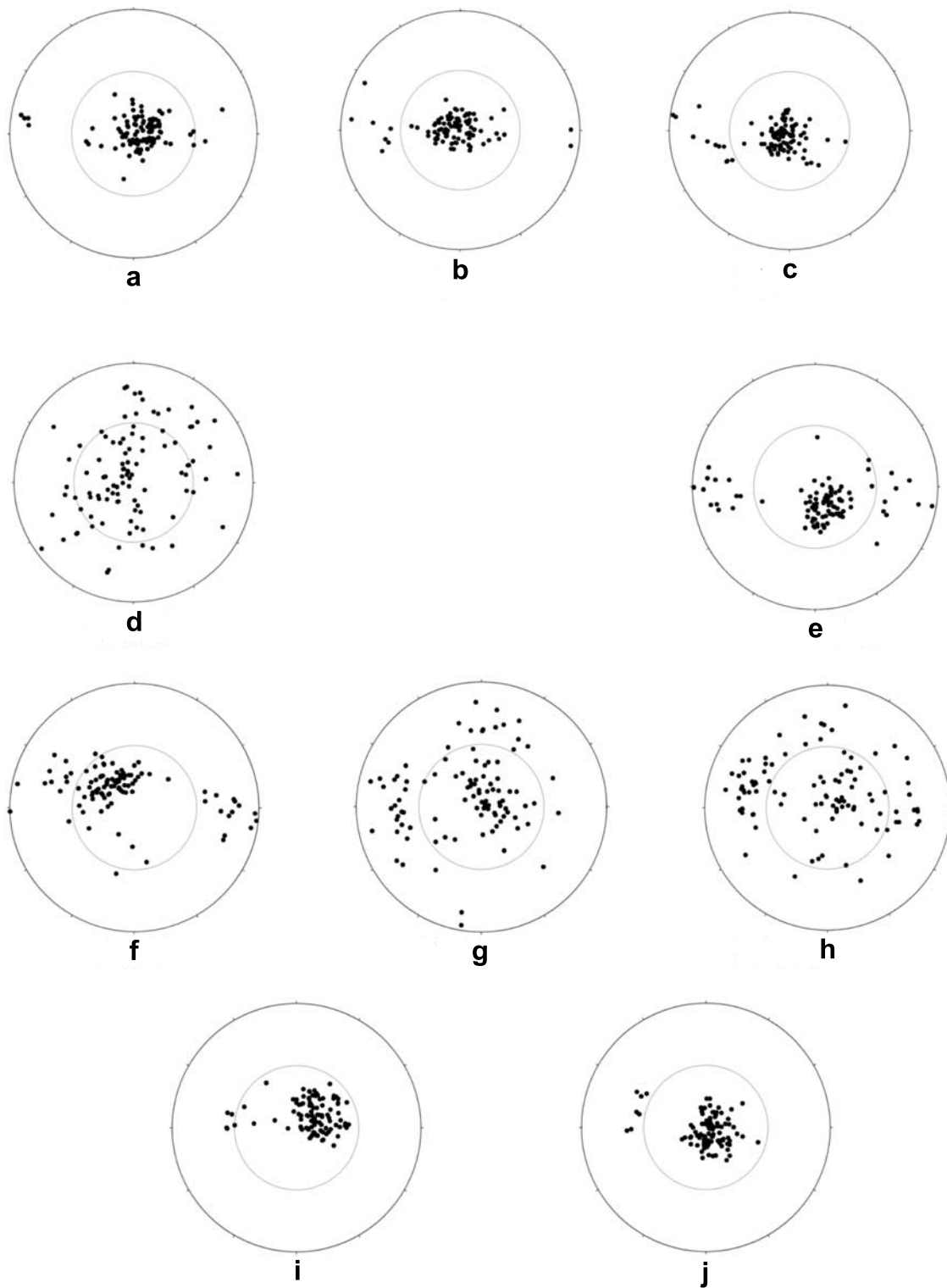


Figure 5



**Figure 6.** Schmidt diagrams (equatorial projections) corresponding to representative sections from the sequence. Portions of these sections are represented in Figure 5. Corresponding  $R$ ,  $I$  and  $S_1-S_3$  are given in Tables 1 and 2. The direction of glacier flow is oriented E–W. The inner circles are at  $45^\circ$  to the vertical axis.

ous changes in crystal texture appear systematically and only in the first centimeter of clean bubbly ice directly in contact with sediment-rich strata. Along with these textural changes, c-axis clustering is significantly decreased, with  $R$

values ranging between approximately 40% and 70% (Figure 7a, Table 1). The corresponding eigenvalues confirm this trend (Figure 7b, Table 1), as indicated by decreasing  $S_1$  and increasing  $I$  values.

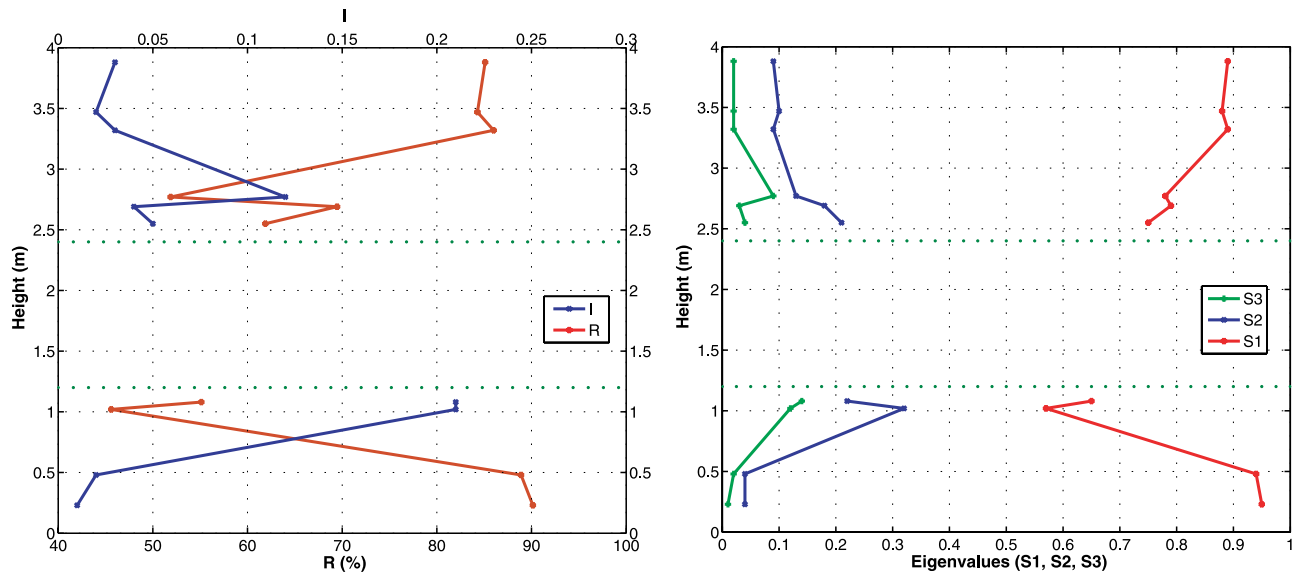


**Figure 7.** Orientation strength  $R$ , isotropy index  $I$ , and eigenvalues  $S_1$ ,  $S_2$ ,  $S_3$  of orientation tensor versus height along the basal ice sequence. The boundaries between the massive and laminated subfacies are marked by thick dotted lines. Mean  $R$ ,  $I$ , and eigenvalues for the englacial facies and the laminated subfacies are given in Table 2.

[22] Some clean ice bands spanned by single ribbons of elongate grains are present within debris-bearing ice layers from the laminated subfacies (Figure 8a). Most of the ice crystals from these one-crystal-thick layers show a pronounced subrectangular outline similar to that at the boundary between clean and debris-rich ice layers. The lattice preferred orientation that we were able to measure in these layers is also similar to that at the boundary zone, though the number of crystals measured was not statistically representative. Undulose extinction and subgrains are, however, generally absent from these crystals.

## 5. Interpretation and Discussion

### 5.1. Recrystallization Regimes

#### 5.1.1. Clean Ice

[23] The strong lattice preferred orientation (LPO) observed in the englacial facies and in the middle part of the clean layers from the laminated subfacies (Figures 6a, 6b, 6c, 6i, and 6j) denotes a preferential alignment of the crystal basal planes close to the plane of maximum shear strain [e.g., Anderton, 1974; Russell-Head and Budd, 1979], revealing a regime dominated by rotation recrystallization. This, according to the dislocation creep regimes introduced by Hirth and Tullis [1992] for different geological materials, would indicate intermediate homologous temperature ( $T/T_m$ , where  $T_m$  is the melting temperature) and strain rate.

[24] It is interesting to note the occasional presence of second, weaker maxima developed a few tens of degrees away from the shear plane and along the shear direction. They resemble those obtained in laboratory shear experiments by Kamb [1972] and Budd [1972] and Duval [1981]. These second maxima were shown to disappear at very large strains ( $>100\%$ ), and thus suggest here the occurrence of moderate to large cumulated strain.

#### 5.1.2. Laminated Subfacies

[25] At the interface between the clean ice layers and the debris-rich ice layers within the laminated subfacies, the association of coarse and lobate crystal textures (Figure 8) with a scattered lattice orientation (Figures 6d, 6e, 6f, 6g, and 6h) is consistent with observations of ice experimentally sheared close to the pressure-melting point [Rigsby, 1960; Huang *et al.*, 1985; Wilson *et al.*, 1996]. Unclustered  $c$ -axis orientations associated with coarse textures have also been found to be common in the basal zone of glaciers and ice sheets, provided that temperature exceeds about  $-12^\circ\text{C}$  [e.g., Kamb, 1959; Rigsby, 1960; Kizaki, 1969; Gow and Williamson, 1976; Duval and Castelnau, 1995; Thorsteinsson *et al.*, 1995]. Such fabrics are generally interpreted as reflecting the occurrence of migration recrystallization, i.e., recrystallization through rapid grain boundary migration and nucleation [e.g., Guillopé and Poirier, 1979; Gottstein and Mecking, 1985]. The formation of “migration fabrics” is not fully understood, but sharp variations of temperature, stress, and strain rate are likely to exert an important control on the observed “lattice loosening” [Anderton, 1974; Gow and Williamson, 1976; Budd and Jacka, 1989]. According to the dislocation creep regimes introduced by Hirth and Tullis [1992], the fabrics observed would have formed at slower strain rates and higher temperatures as compared to the adjacent small crystals in the middle part of the clean ice layers.

[26] Although the latter explanation is often used to account for the development of fabrics at the base of temperate glaciers and ice sheets, it is not consistent with the thermal properties of the studied ice. As noted above, migration recrystallization is acknowledged to require a critical temperature of at least  $-12^\circ\text{C}$  to operate, whereas the present-day temperature at the marginal base of Taylor Glacier is  $-17^\circ\text{C}$  year-round. The question then arises whether such thermal conditions have prevailed during

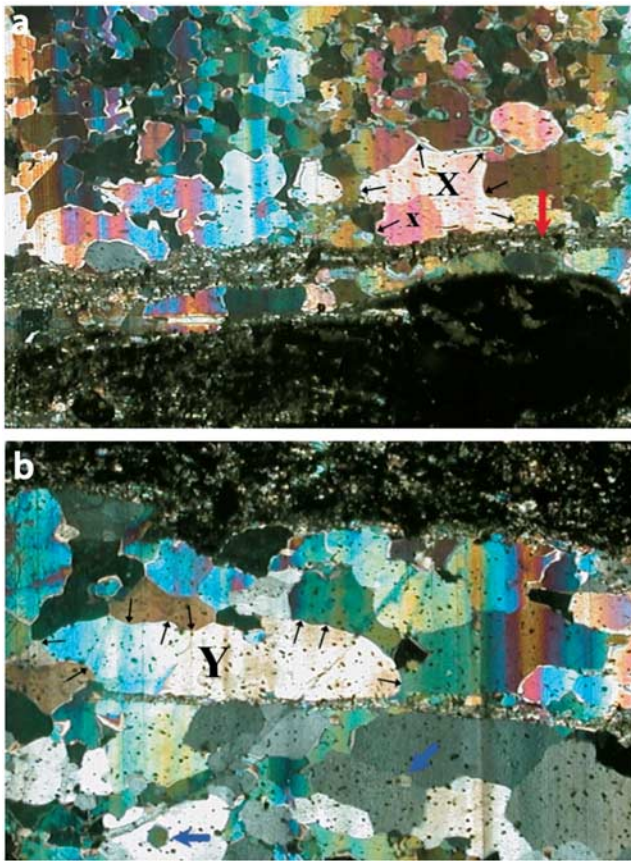


**Figure 8.** Ice crystal ribbons within clean bubbly ice layers at the boundary with debris-rich ice layers (plane polarized colors; height of views: 3.5 cm). The portions of sections presented were sampled at the same stratigraphical level as the portions referred to as *d* and *g*, respectively, in Figure 4. (a) The sharp transition between large interlocked crystals and small equigranular crystals from the middle of a clean ice layer is observable. Grain boundary migration structures (black arrows) are exemplified for one large crystal selected in each section (X and Y). Here x stands for a subgrain in grain X. The red arrow in Figure 8a points to a thin debris-rich lamination isolating a one-crystal-thick ribboned layer. (b) The blue arrows denote spontaneous nucleation (right) at a subgrain boundary as well as (left) within a single crystal.

basal ice formation and deformation, or whether thermal variations could potentially have contributed to the observed fabrics. Detailed gas [Samyn et al., 2005b] and coisotopic [Souchez et al., 2004] analyses have provided in this regard strong arguments for stable and cold temperatures. Hence, although the exact range of potential temperature change is unknown, it is likely that bulk temperature of basal ice has remained well below the freezing point during its development at the base of Taylor Glacier, which would rule out the possibility of temperate formation before the ice was delivered to the margin. The studied ice fabrics would then not simply be inherited from warmer up-glacier conditions, as also supported by sedimentological and glaciological studies suggesting that the presence of thick debris-rich ice at the base of glaciers and ice sheets generally stems from cold

processes, or at least from processes occurring at the thermal transition [Hubbard and Sharp, 1989; Cuffey et al., 2000; Fitzsimons et al., 2001]. Given this, and the fact that the basal temperature at the margin of Dry Valleys glaciers is in equilibrium with the mean annual surface temperature [Chinn, 1991; Robinson, 1984], the possibility of vertical or longitudinal temperature gradients as responsible for the rapid crystal growth is therefore strongly limited in large portions of the snout.

## 5.2. Discontinuous Grain Growth

[27] On all analyzed sections, grain size and aspect ratio are at their largest at the boundaries between debris-free and debris-rich ice layers (examples in Figure 8), and c-axis clustering is minimal there (examples in Figures 6d, 6e, 6f, 6g, and 6h). Bulging of grain boundaries (Figures 8a and 8b) and spontaneous nucleation (as detected in Figure 8b by the presence of small crystals inside much larger ones or at a subgrain boundary) were also observed at these contacts. These processes require particularly high grain boundary mobility in this zone [e.g., Jessell, 1987; Passchier and Trouw, 1996], which implies, as a trigger, a change in bulk energetic balance during the evolution of basal ice.

[28] The ice crystal ribbons observed are consistent with the occurrence of discontinuous grain growth described in various metals and alloys [e.g., Cotterill and Mould, 1976; Cahn, 1983; Gottstein and Mecking, 1985]. As opposed to normal grain growth, this mechanism involves selective growth of specific grains at the expense of the remainder of the matrix. Cahn [1983] and Stöckert and Duyster [1999] distinguished the following characteristic features accounting for the occurrence of discontinuous grain growth: (1) large grains develop from preexisting grains in the initial microstructure; (2) the orientation of these growing grains generally differs from the overall crystallographic preferred orientation; (3) when discontinuous grain growth has occurred, the resulting lattice orientation differs from the initial one; (4) normal grain growth must be inhibited in some places to allow discontinuous grain growth; and (5) a specific temperature threshold must be exceeded for grain growth to proceed.

### 5.2.1. Rheological Contrasts

[29] Insight into the development of the recorded crystals ribbons can be gained from rheological considerations. Crystal energy gradients are necessary for the occurrence of discontinuous grain growth. This implies, in the absence of temperature gradients, fluctuations in the magnitude or direction of stresses. The presence of structural discontinuities within the laminated subfacies should be a determining factor in this regard. Stress heterogeneities generally arise at the contact between rheologically contrasting materials, with strain subsequently tending to localize within the less competent layers [Berthé et al., 1979]. In addition, it is also acknowledged that higher cumulated deformation prior to recrystallization results in faster recrystallization kinetics [Barber, 1985; Radhakrishnan et al., 1998]. This has been ascribed to an increased level of stored energy within the predeformed crystals, thereby providing larger driving force for recrystallization as well as an increased nucleation rate [Radhakrishnan et al., 1998]. Following this line of arguments, we surmise that the discontinuous grain growth found in the laminated subfacies can be accounted for by

the occurrence of strain localization at the interface between the rheologically contrasting ice types from the laminated subfacies.

[30] If the localized deformation hypothesis presented above is valid, the question arises as to which side of the interface experienced the deformation? Very few rheological experiments have been reported on debris-bearing ice, and these have yielded diverse and sometimes contradictory results. Work on different types of debris-bearing ice led to the conclusion that the presence of debris could either strengthen or soften the ice, depending on the concentration, granulometry, and distribution of debris particles [e.g., *Holdsworth*, 1974; *Nickling and Bennett*, 1984; *Echelmeyer and Zhongxiang*, 1987; *Waller and Hart*, 1999; *Fitzsimons et al.*, 2001]. A hint to our question here may be given by strain experiments on basal ice samples from Taylor Glacier. *Lawson* [1996] examined the mechanical behavior of debris-bearing ice versus that of clean glacier ice on centimeter-scale cores. This author showed that below  $-5^{\circ}\text{C}$ , debris-bearing ice reaches (at least two times) higher compressive strengths than clean glacier ice. Although these compressive experiments do not exactly reflect the state of stress at the margin of the glacier (it should correspond to combined pure and simple shear), the observation in question has important rheological implications: at in situ temperature and for centimeter-scale samples, debris-rich ice is likely to accommodate less deformation at the base of the glacier than clean glacier ice. This is consistent with the results of direct shear experiments conducted by *Fitzsimons et al.* [2001] on decimeter-scale basal ice blocks from Sues Glacier, a small dry-based alpine glacier flowing in Taylor Valley. *Fitzsimons* and colleagues showed that at displacement rate ( $\sim 10^{-4}$  mm s $^{-1}$ ) and temperature ( $\sim -17^{\circ}\text{C}$ ) measured at the base of the glacier, debris-rich stratified ice samples are stronger than clean ice samples. If strain were to be localized at the structural interfaces of Taylor Glacier laminated subfacies, it thus appears to be on the clean ice side rather than on the debris-rich side as long as individual layers are 1 cm thick or larger. However, this situation might differ at millimeter scale. *Echelmeyer and Zhongxiang* [1987] conducted structural studies in sub-freezing basal ice ( $\sim -4^{\circ}\text{C}$ ) from Urumqi Glacier Number 1 (China) and found that a significant part of glacier surface motion occurred through discrete shearing localized within subglacial debris-bearing ice. This observation points to a drastic reduction in the creep strength of the debris-rich ice relative to the clean ice at same stress and temperature. *Waller and Hart* [1999] measured similar motion patterns at the base of Russell Glacier, a polythermal glacier from Greenland. For the case of Taylor Glacier, it is therefore plausible that strain was accommodated locally by millimetric debris laminations such as that represented in Figure 8a. This would then allow for stress relaxation, and thereby static recrystallization, within adjacent clean ice layers. Temperature, debris characteristics, and interstitial liquid water content would play a decisive role in this regard.

### 5.2.2. Recrystallization Scenarios

[31] We propose two tectonic scenarios to account for the development of two distinct types of textures and fabrics within the clean ice layers of the laminated subfacies (Figure 9). The first, “static” hypothesis includes the

following events a to c. The second, “dynamic” hypothesis includes the events a, b, and d.

#### 5.2.2.1. Event a

[32] At the margin of the glacier, where the structural manifestations of glaciotectonics are generally important, the clean ice layers from the basal zone are subject to shear stress and deform through dislocation creep, leading to the development of a distinct LPO. This LPO induces low differences in stored strain energy between neighboring crystals, thereby impeding grain boundary migration. Reduction of grain size by polygonization is balanced by grain growth, leading to a stable grain size.

#### 5.2.2.2. Event b

[33] Basal processes lead to the incorporation of debris-bearing ice layers into the bottom sequence. With increasing strain and because of large rheological contrast at the contact between the clean and debris-bearing ice layers, shearing is temporarily localized at such interfaces. Therefore, interfacial ice crystals from the clean layers experience much larger stress variations than those located toward the middle part of the layers. This marks the onset of strong gradients of internal strain energy within the clean ice layers.

#### 5.2.2.3. Event c

[34] In the case where debris-bearing layers are less competent than clean ice layers, strain is first accommodated by debris-bearing ice. Stress therefore relaxes to some extent at the edges of the clean ice layers, i.e., within the interfacial crystals. Differential stress and strain within the clean ice layers then lead to the inception of discontinuous grain growth under thermal conditions allowing migration recrystallization. Nucleation and selective growth of isolated grains favorably oriented with respect to the stress field result in progressive obliteration of initial fabrics at the contact with debris-rich ice. At this contact, increased grain boundary mobility arising from strong energy gradients leads to the development of large, loosely oriented crystals. The overall resulting fabric across the clean bubbly ice layers show two distinct types of fabrics and textures: one is represented in the middle part of the layers by small crystals with a strong LPO and another is represented at the contact with debris-bearing ice by new, large, interlocked, strain free crystals showing a more scattered lattice orientation.

#### 5.2.2.4. Event d

[35] In the case where the debris-rich layers are more competent than the clean ice layers, strain is accommodated by the interfacial ice crystals. Rotation recrystallization is expected to work at its best in these crystals, which should lead to the formation of small grains only slightly misoriented. However, temperature and stress conditions here are such that the imprint of continuous c-axis rotation and polygonization is erased by the effects of nucleation and grain boundary migration which consume grains with their slip planes favorable for easy glide. The nucleation of new grains favorably oriented for deformation induces large differences of stored strain energy between adjacent grains, which in turn further promotes grain boundary migration. Besides, as a result of the strong simple shear component of the flow, grain growth is driven parallel to the main shear plane (which represents the main plane of material transport), thereby leading to pronounced grain elongation. Ribbons of large, interlocked, misoriented crystals finally

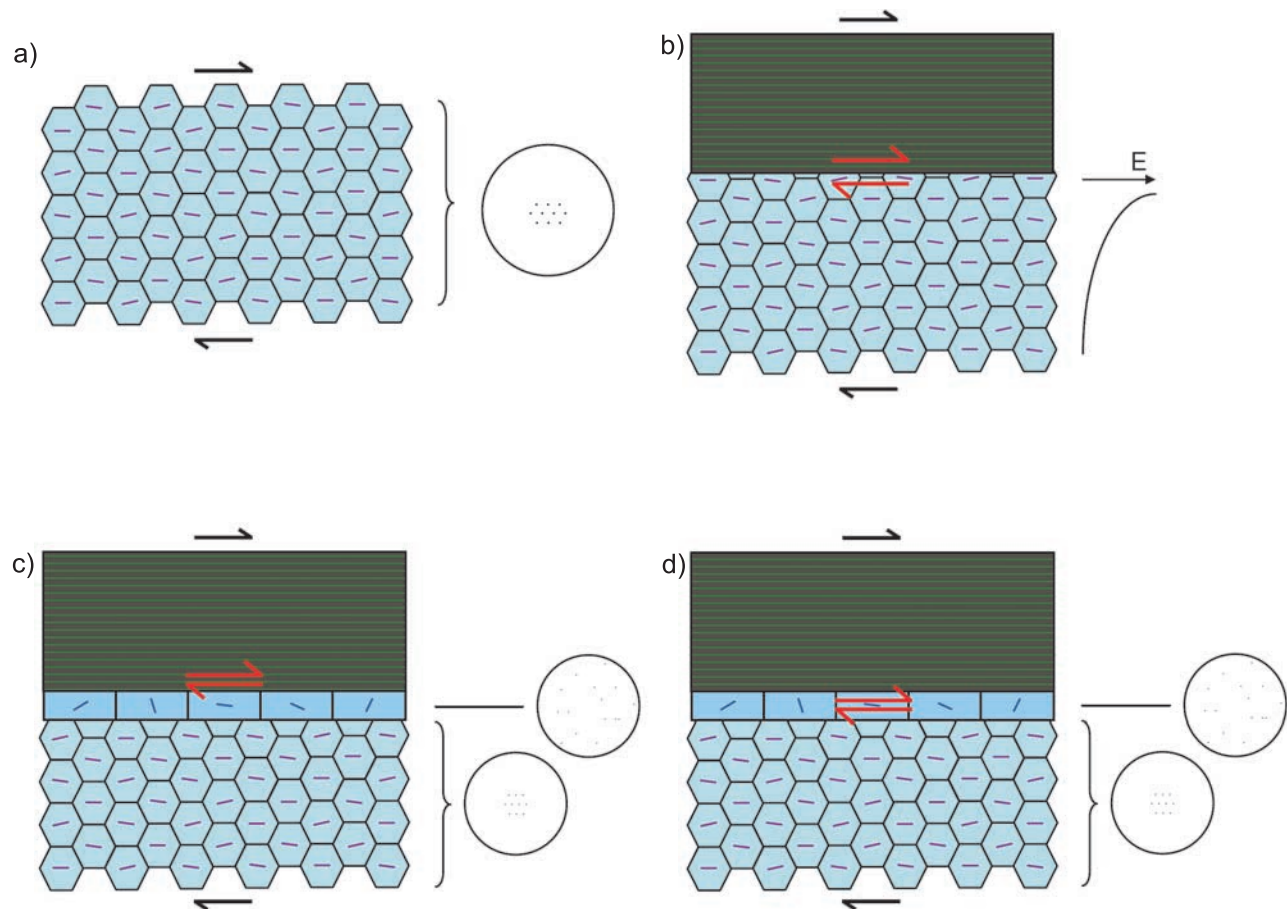


**Figure 9.** Flow and recrystallization patterns for the static and dynamic scenarios discussed in the text: (a) lattice preferred orientation development, (b) building of strain energy ( $E$ ) gradients, (c) debris-bearing ice softer, (d) clean ice softer. Events a-c account for the static scenario; events a, b, and d account for the dynamic scenario.

take over the small, equant grains with a strong LPO at structural interfaces.

[36] According to these scenarios, similar crystallographic fabrics can be produced as a result of different strain histories. In addition, these scenarios can account for the development of contrasting fabrics within the clean ice layers of the stratified facies: (1) strain-induced (or mechanically controlled) fabrics, as is the case for ice present in between the ribbons; and (2) stress-induced (or energetically controlled) fabrics, as is the case for the interfacial ribbons. It should be noted that, strictly speaking and whatever the scenario, the ribboning texture also originates from the occurrence of deformation. But discontinuous recrystallization could initiate in this case only once strain-induced variations in grain size, grain shape or lattice orientation were high enough to provide sufficient driving force for fabric transformation. Despite having different controls, (1) is thus necessary for (2) to occur.

[37] From the above, important feedback mechanisms are expected between stress, accumulated strain, and fabric changes within basal ice. Since recrystallization commonly reduces the free energy of an ice body, the ice crystal ribbons observed in this study may be regarded as buffering structures that reduce the energy stored during deformation near the base of the glacier. It is interesting to note that, despite its

resetting effect on preexisting fabrics, discontinuous grain growth can still be regarded to some extent as a reliable dynamic indicator, since it reflects the occurrence of fluctuating stress and strain conditions in the course of basal ice development.

## 6. Conclusion

[38] Accounting for the relationships between basal ice character and deformation represents an important step toward a more comprehensive and physically based understanding of the flow dynamics and history of ice bodies. In an attempt to formalize basal ice processes at subfreezing temperature, and to assess the potential role played by debris during recrystallization, we document herein the results of crystallographic and structural analyses conducted in cold basal ice ( $\sim -17^{\circ}\text{C}$ ) from the snout of Taylor Glacier (Antarctica). More specifically, we investigate the dynamics underlying rapid grain growth at the boundaries between debris-rich and clean ice layers. Ice crystal ribbons are found to be indicative of the occurrence of discontinuous grain growth at structural interfaces within the basal ice sequence. The following conclusions can be drawn from this study:

[39] 1. Discontinuous grain growth has the potential to alter the intensity and orientation of ice fabrics. This process

led here to the formation of two distinct types of textures and fabrics within stratified basal ice. One type corresponds to fine crystals with a strong lattice preferred orientation (LPO), and the other corresponds to coarse crystal ribbons showing a more scattered lattice orientation. The former occurs at a distance of at least a few centimeters from debris-rich ice, whereas the latter is systematically found at the interface with, or within, debris-bearing ice.

[40] 2. Ice crystal ribbons are likely to play an important role in controlling stress and strain inhomogeneities within basal ice. The fact that such ribbons were observed at the boundaries between debris-rich and clean bubbly ice layers from the stratified facies supports the fact that rheological inhomogeneities control the development of these ribbons.

[41] 3. When migration recrystallization is dominant, both dynamic and static states can induce the growth of ice crystal ribbons. Though no unequivocal indicator was found in this study to clearly distinguish between both recrystallization states, it appears that the ribbon-shaped textures observed at the contact between contrasting ice types are related to zones having undergone significant plastic deformation and strain fluctuations. Besides, previous geochemical arguments have shown that the basal zone temperature has remained stable through the recent past, restricting the thermal conditions under which ribbon growth, and thus migration recrystallization, occurred. This suggests that temperature is not the exclusive factor controlling the onset of migration recrystallization.

[42] 4. Despite its resetting effect on ice crystal textures and lattice orientations, the observation of discontinuous grain growth within cold basal ice sequences may be considered as a reliable strain indicator in that its occurrence requires strong gradients in internal strain energy. Such gradients may be strongly localized within individual basal ice units, as exemplified in this study by drastic fabric changes occurring within a few centimeters in the clean bubbly ice layers of the stratified facies.

[43] 5. Strain partitioning is expected to play a crucial role, at various scales and in many aspects, in the development of compositional and sedimentological layering at the base of cold ice bodies. This is revealed here by the development of various types of lineations, foliations, and structures that directly result from the occurrence of ductile deformation. The spatial consistency of all these structural features is also indicative of pervasive shearing. An analogy between shear flow at cold-based margins and in mylonitic zones can thus be drawn, where large stress gradients and ductile deformation lead to the development of marked planar and linear shape fabrics.

[44] 6. The findings of this study are potentially important with respect to the unresolved question of the origin of coarse textures and multiple-maxima fabrics often found at the base of deep ice sheets (e.g., Byrd, Cape Folger, Law Dome, GISP2, GRIP). They indeed show that the same recrystallization processes may occur at temperate and cold conditions, provided that strain energy is high enough in the latter case. Our work thus challenges the idea that migration fabrics observed in bottom ice from deep ice sheets are exclusive to stagnant, annealed ice. We believe that a better understanding of the effects of temperature, stress, and strain rate fluctuations on grain boundary migration and on the interstitial fluid phase behavior is an important step

toward answering this question. More experimental work on the strength of debris-bearing ice is also needed to decipher the effect of strain localization on fabric anisotropy at the base of glaciers and ice sheets. Another promising, though calculation consuming, approach to simulate the deformation and texture development of basal ice in dynamic conditions is the N-sites model introduced by *Lebensohn* [2001] for viscoplastic materials, allowing detailed computation of heterogeneous stress and strain states within single grains in the polycrystal.

[45] **Acknowledgments.** We thank Antarctica New Zealand for providing the logistical field support for this study. The Marsden Fund of the Royal Society of New Zealand and the University of Otago provided financial support. This work is also a contribution to the Belgian Scientific Program on Antarctica (OSTC-SSTC). D.S. acknowledges support of a FRIA grant (National Science Foundation, Belgium) by the time the present work was conducted. Financial assistance from FNRS (National Scientific Foundation, Belgium) also allowed D.S. to use the facilities of the Ice and Climate Group from the Niels-Bohr Institute (University of Copenhagen, Denmark). R. Lorrain is thanked for his comments on an early version of this paper. B. Hubbard, P. Knight, and R. Waller are also thanked for their constructive reviewing work.

## References

- Alley, R. B. (1988), Fabrics in polar ice sheets: Development and prediction, *Science*, 240(4851), 493–495, doi:10.1126/science.240.4851.493.
- Alley, R. B., J. H. Pehrepezo, and C. R. Bentley (1986), Grain growth in polar ice: II. Application, *J. Glaciol.*, 32(112), 425–433.
- Alley, R. B., A. J. Gow, S. J. Johnsen, J. Kipfstuh, D. A. Meese, and T. Thorsteinsson (1995), Comparison of deep ice cores, *Nature*, 373(6513), 393–394, doi:10.1038/373393b0.
- Anderton, P. W. (1974), Ice fabrics and petrography, Meserve Glacier, Antarctica, *J. Glaciol.*, 13(68), 285–306.
- Azuma, N. (1994), A flow law for anisotropic ice and its implication to ice sheets, *Earth Planet. Sci. Lett.*, 128(3–4), 601–614, doi:10.1016/0012-821X(94)90173-2.
- Baker, R. W. (1978), The influence of ice-crystal size on creep, *J. Glaciol.*, 21(85), 485–500.
- Barber, D. J. (1985), Dislocations and microstructures, in *Preferred Orientation in Deformed Metals and Rocks: An Introduction to Modern Texture Analysis*, edited by H.-R. Wenk, pp. 149–182, Elsevier, Orlando, Fla.
- Berthé, D., P. Choukroune, and P. Jegouzo (1979), Orthogneiss, mylonite and non coaxial deformation of granites: The example of the South Armorican Shear Zone, *J. Struct. Geol.*, 1, 31–42, doi:10.1016/0191-8141(79)90019-1.
- Budd, W. F. (1972), The development of crystal orientation fabrics in moving ice, *Z. Gletscherkd. Glazialgeol.*, 8(1–2), 65–105.
- Budd, W. F., and T. H. Jacka (1989), A review of ice rheology for ice-sheet modeling, *Cold Reg. Sci. Technol.*, 16, 107–144, doi:10.1016/0165-232X(89)90014-1.
- Cahn, R. W. (1983), Secondary recrystallization, in *Physical Metallurgy*, edited by R. W. Cahn and P. Haasen, pp. 1658–1671, Elsevier, Amsterdam.
- Calkin, P. E. (1974), Subglacial geomorphology surrounding the ice free valleys of southern Victoria Land, Antarctica, *J. Glaciol.*, 13(69), 415–429.
- Castelnaud, O., H. Shoji, H. Milsch, A. Mangeney, P. Duval, A. Miyamoto, K. Kawada, and O. Watanabe (1998), Anisotropic behavior of GRIP ices and flow in central Greenland, *Earth Planet. Sci. Lett.*, 154(1–4), 307–322, doi:10.1016/S0012-821X(97)00193-3.
- Chinn, T. J. H. (1991), Polar glacier margin and debris features, *Mem. Soc. Geol. Ital.*, 46, 25–44.
- Cotterill, P., and P. R. Mould (1976), *Recrystallization and Grain Growth in Metals*, Surrey Univ. Press, London.
- Cuffey, K. M., H. Conway, A. Gades, B. Hallet, C. F. Raymond, and S. Whitlow (2000), Deformation properties of subfreezing glacier ice: Role of crystal size, chemical impurities, and rock particles inferred from in-situ measurements, *J. Geophys. Res.*, 105(B12), 27,895–27,915, doi:10.1029/2000JB900271.
- Durand, G., A. Persson, D. Samyn, and A. Svensson (2008), Relation between neighbouring grains in the upper part of the NorthGRIP ice core — Implications for rotation recrystallization, *Earth Planet. Sci. Lett.*, 265(3–4), 666–671, doi:10.1016/j.epsl.2007.11.002.
- Duval, P. (1981), Creep and fabrics of polycrystalline ice under shear and compression, *J. Glaciol.*, 27(95), 129–140.

- Duval, P., and O. Castelnau (1995), Dynamic recrystallization of ice in polar ice sheets, *J. Phys. IV*, 5, 197–205, doi:10.1051/jp4:1995317.
- Echelmeyer, K., and W. Zhongxiang (1987), Direct observations of basal sliding and deformation of basal drift at sub-freezing temperatures, *J. Glaciol.*, 33(113), 83–98.
- Fitzsimons, S. J., K. J. McManus, P. Sirota, and R. D. Lorrain (2001), Direct shear tests of materials from a cold glacier: Implications for landform development, *Quat. Int.*, 86(1), 129–137, doi:10.1016/S1040-6182(01)00055-6.
- Gottstein, G., and H. Mecking (1985), Recrystallization, in *Preferred Orientation in Deformed Metals and Rocks: An Introduction to Modern Texture Analysis*, edited by H.-R. Wenk, pp. 183–218, Elsevier, Orlando, Fla.
- Gow, A. J. (1969), On the rates of growth of grains and crystals in south polar firn, *J. Glaciol.*, 8(53), 241–252.
- Gow, A. J., and T. Williamson (1976), Rheological implications of the internal structure and crystal fabrics of the West Antarctic ice sheet as revealed by deep core drilling at Byrd Station, *Rep. 76-35*, Cold Reg. Res. and Lab, Hanover, N. H.
- Guillopé, M., and J. P. Poirier (1979), Dynamic recrystallization during creep of single-crystalline halite: An experimental study, *J. Geophys. Res.*, 84(B10), 5557–5567, doi:10.1029/JB084iB10p05557.
- Hirth, G., and J. Tullis (1992), Dislocation creep regimes in quartz aggregates, *J. Struct. Geol.*, 14, 145–159, doi:10.1016/0191-8141(92)90053-Y.
- Hockey, B. (1970), An improved coordinate system for particle shape representation, *J. Sed. Petrol.*, 40, 1054–1056.
- Holdsworth, G. (1974), Meserve Glacier, Wright Valley, Antarctica: Part I. Basal processes, *Rep. 37*, Ohio State Univ. Inst. of Polar Stud., Columbus, Ohio.
- Huang, M., M. Ohtomo, and G. Wakahama (1985), Transition in preferred orientation of polycrystalline ice from repeated recrystallization, *Ann. Glaciol.*, 6, 263–264.
- Hubbard, B., and M. Sharp (1989), Basal ice formation and deformation: A review, *Prog. Phys. Geogr.*, 13(4), 529–558, doi:10.1177/030913338901300403.
- Hubbard, A., W. Lawson, B. Anderson, B. Hubbard, and H. Blatter (2004), Evidence for extensive sub-glacial ponding across the tongue of Taylor Glacier, Antarctica, *Ann. Glaciol.*, 39, 79–84, doi:10.3189/172756404781813970.
- Jessell, M. W. (1987), Grain-boundary migration microstructures in a naturally deformed quartzite, *J. Struct. Geol.*, 9, 1007–1014, doi:10.1016/0191-8141(87)90008-3.
- Kamb, B. (1972), Experimental recrystallization of ice under stress, in *Flow and Fracture of Rocks*, *Geophys. Monogr. Ser.*, vol. 16, edited by H. C. Heard et al., pp. 211–241, AGU, Washington, D. C.
- Kamb, W. B. (1959), Ice petrofabric observations from Blue Glacier, Washington, in relation to theory and experiment, *J. Geophys. Res.*, 64(11), 1891–1909, doi:10.1029/JZ064i011p01891.
- Kizaki, K. (1969), Ice-fabric study of the Mawson region, East Antarctica, *J. Glaciol.*, 8(53), 253–276.
- Langway, C. C., H. Shoji, and N. Azuma (1988), Crystal size and orientation patterns in the Wisconsin-age ice from Dye 3, Greenland, *Ann. Glaciol.*, 10, 109–115.
- Lawson, D. E. (1979), Sedimentological analysis of the western terminus region of the Matanuska Glacier, *Rep. 79-9*, Cold Reg. Res. and Lab., Hanover, N. H.
- Lawson, W. (1996), The relative strengths of debris-laden basal ice and clean glacier ice: Some evidence from Taylor Glacier, Antarctica, *Ann. Glaciol.*, 23, 270–276.
- Lebensohn, R. A. (2001), A N-site modeling of a 3D viscoplastic polycrystal using Fast Fourier Transform, *Acta Mater.*, 49, 2723–2737, doi:10.1016/S1359-6454(01)00172-0.
- Means, W. D. (1983), Microstructure and micromotion in recrystallization flow of octachloropropane: A first look, *Geol. Rundsch.*, 72, 511–528, doi:10.1007/BF01822080.
- Nickling, W. G., and L. Bennett (1984), The shear strength characteristics of frozen coarse granular debris, *J. Glaciol.*, 30(106), 348–357.
- Passchier, C. W., and R. A. J. Trouw (1996), *Microtectonics*, Springer, Berlin.
- Poirier, J.-P. (1985), *Creep of Crystals*, 260 pp., Cambridge Univ. Press, Cambridge, U. K.
- Radhakrishnan, B., G. B. Sarma, and T. Zacharia (1998), Monte Carlo simulation of deformation substructure evolution during recrystallization, *Scr. Mater.*, 39(12), 1639–1645, doi:10.1016/S1359-6462(98)00376-5.
- Ralph, B. (1990), Grain growth, *Mater. Sci. Technol.*, 6, 1139–1144.
- Rigsby, G. P. (1960), Crystal orientation in glacier and experimentally deformed ice, *J. Glaciol.*, 3(27), 589–606.
- Robinson, P. H. (1984), Ice dynamics and thermal regime of Taylor Glacier, South Victoria Land, Antarctica, *J. Glaciol.*, 30(105), 153–160.
- Russell-Head, D. S., and W. F. Budd (1979), Ice-sheet flow properties derived from bore-hole shear measurements combined with ice core studies, *J. Glaciol.*, 24(90), 117–130.
- Samyn, D. (2005), Structural and geochemical analysis of basal ice from Taylor Glacier, Dry Valleys, Antarctica: On the role and behaviour of the interstitial fluid phase, Ph.D. thesis, 206 pp., Univ. Libre de Bruxelles, Brussels.
- Samyn, D., A. Svensson, S. J. Fitzsimons, and R. Lorrain (2005a), Ice crystal properties of amber ice and strain enhancement at the base of cold Antarctic glaciers, *Ann. Glaciol.*, 40, 185–190, doi:10.3189/172756405781813618.
- Samyn, D., S. J. Fitzsimons, and R. Lorrain (2005b), Strain-induced phase changes within cold basal ice from Taylor Glacier (Antarctica) indicated by textural and gas analyses, *J. Glaciol.*, 51(175), 611–619, doi:10.3189/172756505781829098.
- Souchez, R. A., and R. D. Lorrain (1991), *Springer Series in Physical Environment*, vol. 8, 207 pp., Springer, Berlin.
- Souchez, R., D. Samyn, R. Lorrain, F. Pattyn, and S. Fitzsimons (2004), An isotopic model for basal freeze-on associated with subglacial upward flow of pore water, *Geophys. Res. Lett.*, 31, L02401, doi:10.1029/2003GL018861.
- Stöckhert, B., and J. Duyster (1999), Discontinuous grain growth in recrystallised vein quartz—Implications for grain boundary structure, grain boundary mobility, crystallographic preferred orientation, and stress history, *J. Struct. Geol.*, 21, 1477–1490, doi:10.1016/S0191-8141(99)00084-X.
- Svensson, A., K. G. Schmidt, D. Dahl-Jensen, S. J. Johnsen, Y. Wang, J. Kipfstuhl, and T. Thorsteinsson (2003), Properties of ice crystals in NorthGRIP late-to middle- Holocene ice, *Ann. Glaciol.*, 37, 113–118, doi:10.3189/172756403781815636.
- Thorsteinsson, T., J. Kipfstuhl, H. Eicken, S. J. Johnsen, and K. Fuhrer (1995), Crystal size variations in Eemian-age ice from the GRIP ice core, central Greenland, *Earth Planet. Sci. Lett.*, 131(3–4), 381–394, doi:10.1016/0012-821X(95)00031-7.
- Tison, J.-L. (1994), Diamond wire-saw cutting technique for investigating textures and fabrics of debris-laden ice and brittle ice, *J. Glaciol.*, 40(135), 410–414.
- Urai, J. L., W. D. Means, and G. S. Lister (1986), Dynamic recrystallization of minerals, in *Mineral and Rock Deformation: Laboratory Studies—The Paterson Volume*, *Geophys. Monogr. Ser.*, vol. 36, edited by B. E. Hobbs and H. C. Heard, pp. 161–199, AGU, Washington, D. C.
- Vernon, R. H. (1981), Optical microstructure of partly recrystallized calcite in some naturally deformed marbles, *Tectonophysics*, 78, 601–612, doi:10.1016/0040-1951(81)90031-7.
- Wallbrecher, E. (1978), Ein clusterverfahren zur richtungsstatistischen analyse tektonischer daten, *Geol. Rundsch.*, 67, 840–857, doi:10.1007/BF01983240.
- Waller, R. I., and J. K. Hart (1999), Mechanisms and patterns of motion associated with the basal zone of an arctic glacier: Russell Glacier, Greenland, *J. Glacial Geol. Geomorphol.*, 21, 1–20.
- Weiss, J., J. Vidot, M. Gay, L. Arnaud, P. Duval, and J.-R. Petit (2002), Dome Concordia ice microstructure: Impurities effect on grain growth, *Ann. Glaciol.*, 35, 552–558, doi:10.3189/172756402781816573.
- Wilson, C. J. L., Y. Zhang, and K. Stüwe (1996), The effects of localized deformation on melting processes in ice, *Cold Reg. Sci. Technol.*, 24, 177–189, doi:10.1016/0165-232X(95)00024-6.
- Wilson, C. J. L., D. S. Russell-Head, and H. M. Sim (2003), The application of an automated fabric analyzer system to the textural evolution of folded ice layers in shear zones, *Ann. Glaciol.*, 37, 7–17, doi:10.3189/172756403781815401.
- Woodcock, N. H. (1977), Specification of fabric shapes using an eigenvalue method, *Geol. Soc. Am. Bull.*, 88, 1231–1236, doi:10.1130/0016-7606(1977)88<1231:SOFSUA>2.0.CO;2.

S. J. Fitzsimons, Department of Geography, University of Otago, P.O. Box 56, Dunedin, 9001, New Zealand.

D. Samyn, Department des Sciences de la Terre et de l'Environnement, Faculté des Sciences, Université de Bruxelles, B-1050 Brussels, Belgium. (desamyn@ulb.ac.be)

A. Svensson, Department of Geophysics, Niels Bohr Institute for Astronomy, Geophysics, and Physics, University of Copenhagen, Copenhagen, D-2100, Denmark.